HEATING DISTRIBUTIONS OF THE SPALLATION NEUTRON SOURCE

F. C. Difilippo and L. A. Charlton
Oak Ridge National Laboratory*
P.O. Box 2008, MS-6363
Oak Ridge, Tennessee 3783 l-6363

"The submitted manuscript has been authored by a contractor of the U.S. Government under contract DE-AC05-96OR22464. Accordingly, the U.S. Government retains a nonexclusive, royalty-free license to publish or reproduce the published form of this contribution, or allow others to do so, for U.S. Government purposes."

Full paper submitted for publication and oral presentation, *AccApp '99*, Long Beach, CA, November 14–18, 1999.

*Research sponsored by the Oak Ridge National Laboratory managed by Lockheed Martin Energy Research Corporation for the U.S. Department of Energy under contract No. DE-AC05-96OR22464.

HEATING DISTRIBUTIONS IN THE TARGET OF THE SPALLATION NEUTRON SOURCE

Felix C. Difdippo
Oak Ridge National Laboratory
P. 0. Box 2008
Oak Ridge, TN 37x31-6363
(423) 574.6188

ABSTRACT

Detailed calculation of the heat distributions in the structural parts of the target (Hg) and the target itself were made with realistic proton profiles. Preliminary current profiles of the protons coming from the accumulator ring, calculated and parameterized by the Brookhaven

II. FIT OF THE PROTON CURRENT

Figure 1 is the contour plot of the current distribution of Table 1 as function of x and y. The Contours of equal intensity are, in general, quasi rectangles with semicircular corners and gaussian profiles for the intensity as function of x and y. Thirty six contours were used to discretized the source: the first is for the intensity I_0 (rectangle 4 x_0 y_0), the rest were calculated numerically as solutions of f (x, y) = I, I in steps of 0.05 * I_0 for I > 0.1 * I_0, I in steps of 0.01* I_0 for I > 0.01 * I_0, I in steps of 0.002* I_0 for I > 0.001 * I_0 and I in steps of 0.0005* I_0 for I > 0.0001 * I_0, the last contour correspond to I = 0.00001* I_0 In this process, the area within each contour was determined also numerically.

With the area, A,, of the contours known, the areas of the ellipses are also known, $A_c = \pi a_c b_c$. The additional constraint that the set of ellipses has to have a common value for the ratio b_c/a_c determines a, and b_c. Figure 2 shows the result for the average differences between the real source and the elliptical approximations as a function of the ratio b_c/a_c, the best results are for the ratio equal to 0.26 (eccentricity e = 0.965609). Although the important central region has the right value for the proton current, the general average difference is rather large. Figure 3 shows the contour plot of the optimal elliptical approximation to the real source of Fig. 1.

III. DEFINITION OF THE MATERIAL REGIONS FOR THE TALLIES

The fact that the source is now described with contours of equal intensities allows one to circumvent the difficulties of obtaining statistically meaningful 3-D heat distributions. Because the source is almost constant within the elliptical rings, the average heat in each ring as function of z is representative of the real heat distribution. We used then a subset of the ellipses describing the source to define material cells for the target, Hg. These cells have the shape of a cylindrical shell with elliptical cross section: fourteen elliptical cylinders were chosen, the first two correspond to the region with relative (to I_0) intensity 1.0, the rest in decrement of 0.1 step down to 0.1, then relative intensities 0.05, 0.01 and the last 0.001. Cylindrical shell 15 corresponds to the material region beyond cylinder 14 (i.e., I < 0.001* I_0). Figure 4 shows the cross section of the 15 rings that correspond to the bulk region of the Hg target.

N. HEAT DISTRIBUTIONS

Total heat distribution tallies were calculated for each one of the cylindrical shells as a function of the distance to the border of the Hg inside the nose of the target [3] (where the proton beam starts to interact with the massive part of the Hg). Strictly speaking we should present the results as function of z and either an index related to each one of the elliptical rings or the semi-major axis (a) of the ring. But all the x and y that satisfy

$$a = \sqrt{x^2} + \frac{y^2}{1-e^2} \qquad (1),$$

where e=0.965609 is the common value of the eccentricity, belong to an elliptical region (in x,y) with almost constant proton current so we can argue that the average heat for the ring is near the real heat for those x and y that satisfy Eq. (1). In this sense results for the LAHET calculated heat (produced by particles with energies above 20 MeV) shown in Fig. 5 are considered 3-D heat distributions.

A thin region of Hg (the outer nose, the region of the target that first interact with the protons) requires an independent flow outside the inner nose and the bulk region of the Hg target. Also the entire Hg is inside a stainless steel (ss) jacket that is water-cooled. From the point of view of the proton beam then, there are six walls with which the beam interacts first in the following order: ss wall 1, water wall, ss wall 2, ss wall 3, Hg wall and ss wall 4. Because of the high value of the heat dissipation, values and gradients are very important in these regions. The description of these material cells in terms of the same set of cylindrical shells that describe the source allows one to follow the heat distribution as a function of x and y (in this case the walls are thin so z is given by the x y position on the surfaces that bound the walls). Figure 6 shows the heat distributions for the six walls as a function of a (semi-major axis), for each (x,y) Eq. (1) gives the value of a to read the heat in Fig. 6. The heat distributions follow the proton distribution, also shown in Fig. 6.

V. CONCLUSIONS

Due to present limitations in the description of the proton source in the LAHET code, realistic beam profiles have to be approximated by current distributions in a set of nested elliptical shells. Taking advantage of this constraint, material cells were defined to calculate heat tallies that follow the geometry of the source, in this way two dimensional averages are representative of the real 3-D heat distribution. The idea is obviously not restricted to the elliptical case and can be used for other sets of surfaces. One byproduct of the approach is a description

of the gradient of the heat in the x,y directions. A more exact method is necessary for SNS design calculations. Such a method is now being developed.

REFERENCES

1. T. McManamy, "Proton Beam Intensity Models for Use with Target Design," Brookhaven National Laboratory, Personal Communication, Oct. 2,1998.

2. R.E. Prael and L. Lichtenstein, "User Guide to LCS: The Lahet System," Los Alamos National Laboratory, LA-UR-89-3014 (September 1989).

3. See for example description of the entire target station in "*Energy* Dissipation in the Target Station of *the Spallation Neutron* Source," F. C. Difilippo and L.A. Charlton, *Proc. Int. Conf.* on Math. and *Comp.*, Reactor Physics and Environmental Analysis in Nuclear Applications, American Nuclear Society, Madrid, Spain, Sept 27-30, 1999.

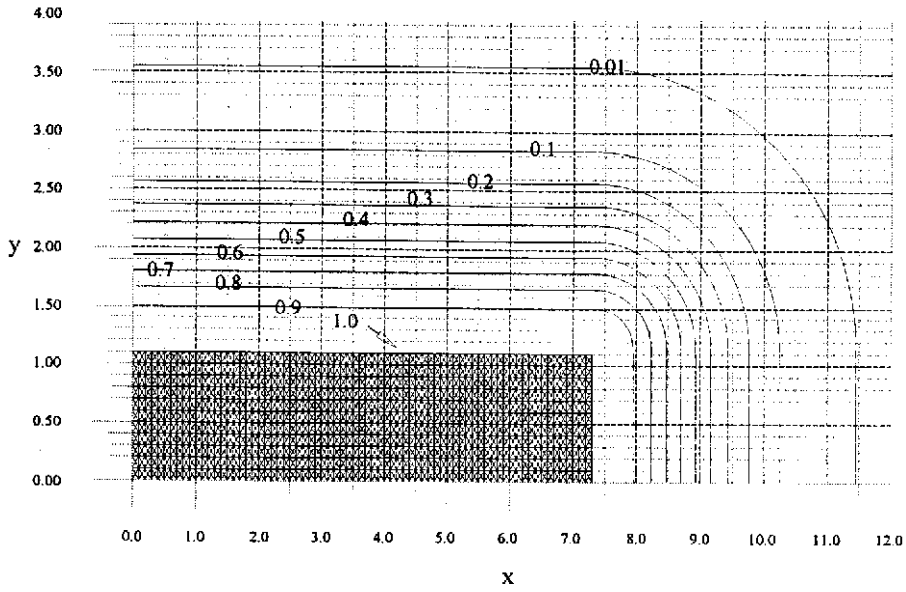
4.00
3.50
3.00
2.50
2.00
1.50
1.00
0.50
0.00
y
0.0
1.0
2.0
3.0
4.0
5.0
6.0
7.0
8.0
9.0
10.0
11.0
12.0
x
0.01
0.1
0.2
0.3
0.4
0.5
0.6
0.7
0.8
0.9
1.0

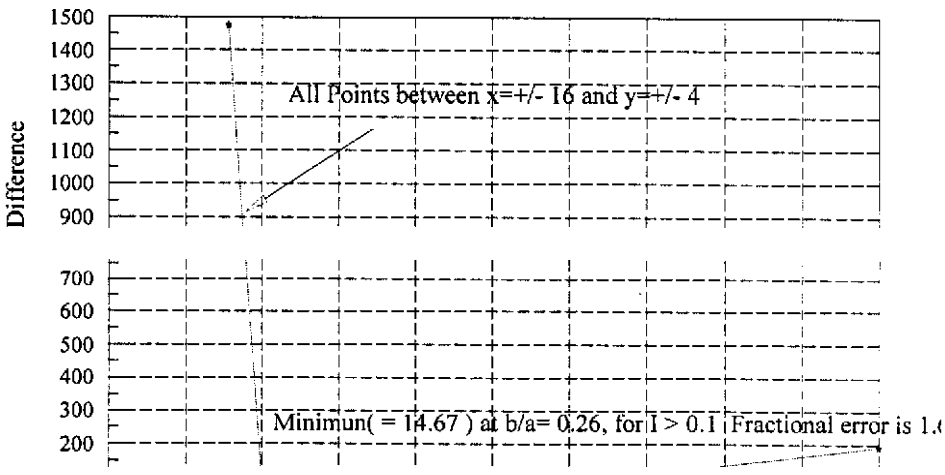
Difference
1500
1400
1300
1200
1100
1000
900
700
600
500
400
300
200
All Points between x=+/- 16 and y=+/- 4
Minimun(= 14.67) at b/a= 0.26, for 1 > 0.1 Fractional error is 1.

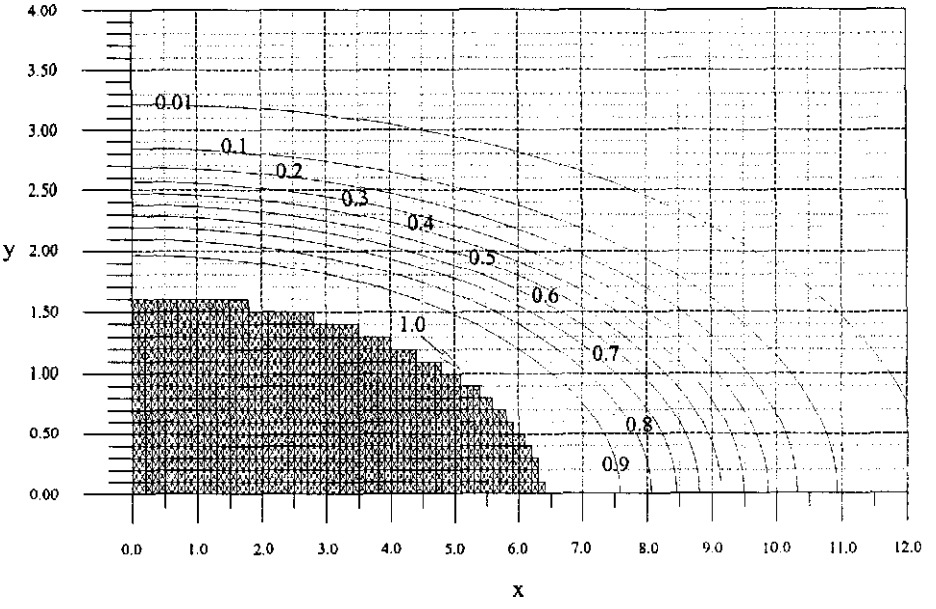

Fig. 3. Contour plot of the optimized elliptical approximation to the proton source of Fig. 1.

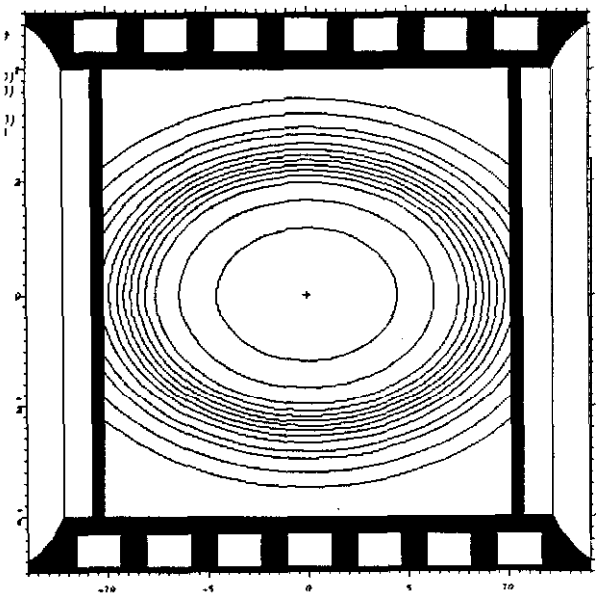

Fig, 4. Regions for tallies in the bulk region of the Hg target. The ellipses define cylindrical shells that correspond to regions of approximately constant proton current.

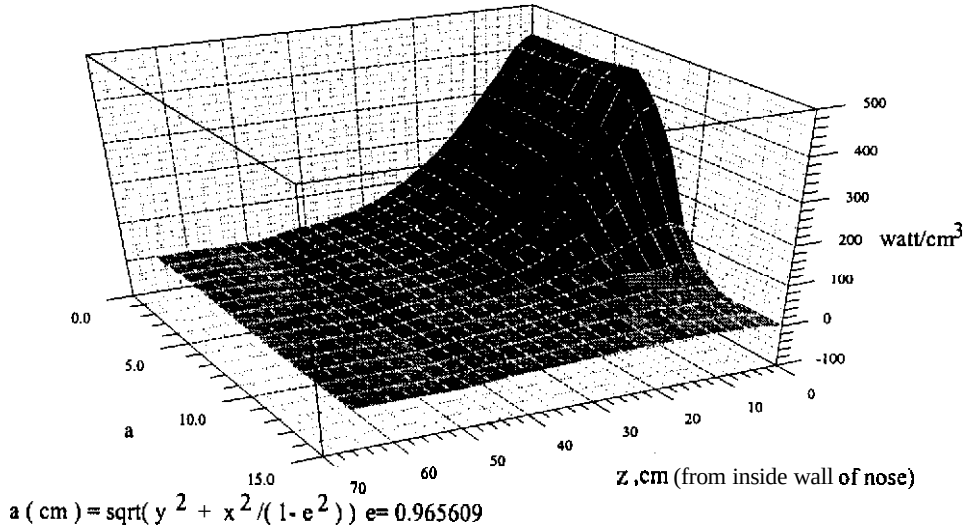

Fig. 5. LAHET heat (for processes with E > 20 MeV) as function of z and a, the semi-major axis of each elliptical ring. All the x and y satisfying the equation are within a ring with almost constant proton current so the average value is representative of the heat density at x,y.

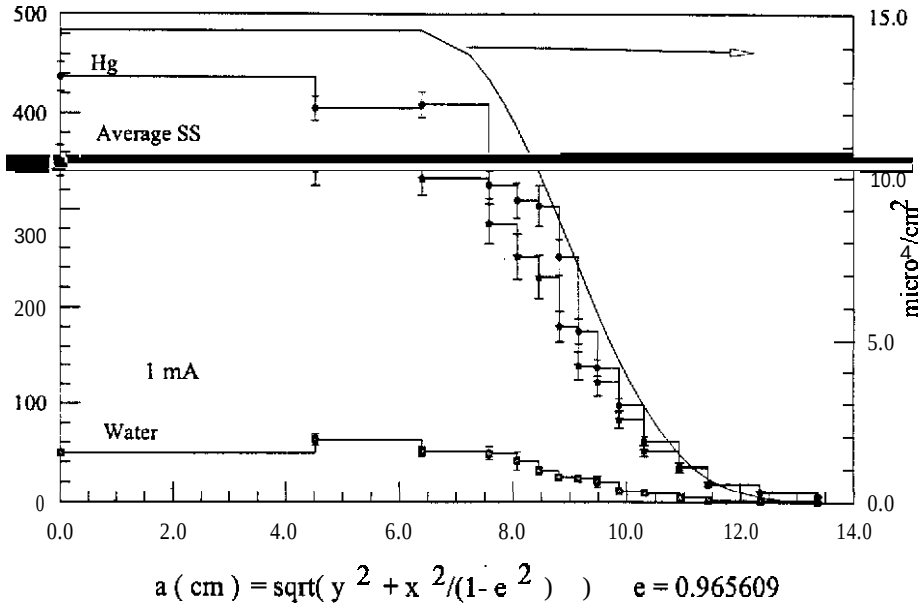

Fig. 6. LAHET heat distributions for the first six walls that interact with the proton beam: four stainless steel (shown as an average), water and the Hg of the outside nose. Correspond to the distribution of Fig. 3 at 1 mA, 1 GeV.